Molar and Excess Volumes of Liquid In–Sb, Mg–Sb, and Pb–Sb Alloys

Allen R. Hansen and Mark A. Kaminski

Department of Chemical Engineering, University of Illinois, Urbana, Illinois 61801

Charles A. Eckert*

School of Chemical Engineering, Georgia Institute of Technology, Atlanta, Georgia 30332-0100

By a direct Archimedes' technique, volumetric data were obtained for liquid In, Mg, Pb, and Sb and mixtures of In–Sb, Mg–Sb, and Pb–Sb. The excess volumes for the alloys studied are presented and discussed.

Introduction

Though much excess enthalpy and Gibbs energy data are available for liquid metal mixtures, corresponding excess volume information is often lacking or of poor quality. The excess volume, or volume change on mixing (defined by eq 1), is a

$$v^{EX} = v_{MIX} - x_A v_A - x_B v_B \quad (1)$$

measure of solution nonideality that is relatively easy to obtain and should be utilized more extensively in thermodynamic solution modeling. This is particularly true for metallic mixtures since there is a significant sensitivity of mobile valence electrons, and subsequent metallic properties, to the density of the melt. Therefore, further development of thermodynamic solution models that address the physics of liquid metal alloys should depend strongly upon the availability of adequate molar and excess volume data.

Molar and excess volumes for liquid In–Sb, Mg–Sb, and Pb–Sb alloys are presented here, which supplement information published previously by this group (*1*). Volumetric data were obtained for temperatures near the liquidus up to as much as 1000 °C and for concentrations spanning the entire accessible range.

Experimental Section

Details of the experimental equipment and procedures have been described elsewhere (*1*); highlights are reviewed briefly. Figure 1 illustrates the experimental chamber in which a direct Archimedes' technique was utilized to determine the density of the melt. In this technique, the buoyant force exerted on an inert, calibrated bob submerged in the melt is measured by an electronic balance and the density calculated by the equation

$$\rho = (F_b + \gamma)/(V_B + V_W) \quad (2)$$

where V_B and V_W are the volumes of the bob (corrected for thermal expansion (*2*)) and submerged wire, respectively. The buoyant force, F_b, is equal to the difference between the weights of the bob before and after its immersion into the melt. The surface tension correction, γ, which accounts for the force exerted on the suspension wire by the surface of the melt, was ignored since such thin wires were used (0.25-mm diameter).

All experiments were performed under an argon atmosphere so that oxidation was not a problem. Temperatures were measured with a chromel–alumel thermocouple submersed in the melt and were kept low enough to make evaporation insignificant. The thermocouple was calibrated by measuring the freezing points of silver, lead, and zinc and was found to be accurate to better than ±5 °C. The electronic balance was read to the nearest 1 mg.

Alloy concentrations were changed by adding metal pieces to the melt through a stainless steel tube just above the crucible. The tube extended up and out of the apparatus where it was connected to a Pyrex chamber that was evacuated and purged with argon before introducing the metal pieces into the system. Stirring was achieved by moving the crucible platform up and down as the bob remained stationary. Metal additions made to Mg–Sb alloys were performed especially slowly since the favorable formation of a high melting point compound (Mg_3Sb_2) evolved significant heat and took a short time to dissolve into the melt.

Due to the temperature and the aggressive nature of liquid metals, the compatibility of materials is extremely important. Tungsten and tantalum bobs (approximately 10 cm^3) suspended by tungsten wire performed well in the three alloys studied. The tantalum bob was used only for the Mg–Sb alloys. Alumina crucibles, which were used to contain the melt, also worked well. When a magnesium alloy was being studied, however, the quartz thermocouple sleeve had to be replaced by a molybdenum-tipped sleeve and the quartz furnace tube gradually deteriorated.

All of the metals used were obtained from Aldrich Chemical Co. and, except for Sb, had purities of at least three nines. The antimony was 99.8% pure.

Results and Discussion

The densities and molar volumes measured are presented in Table I. Within experimental error, the molar volume data may be represented by linear least-squares fits as shown in Table II. Some concentrations of the In–Sb system could not be obtained because of adverse interactions between the melt and the surface of the bob. Also, Mg–Sb data in the range x_{Mg} = 0.5–0.7 were unobtainable due to the high melting point compound. Figures 2–4 show the excess volumes determined from this data along with least-squares-fit curves. A three-parameter Redlich–Kister-type equation was used to represent the excess volume data:

$$v^{EX} = x_A x_B(A + B(x_A - x_B) + C(x_A - x_B)^2) \quad (3)$$

The constants to be used in eq 3 are tabulated in Table III and are relatively temperature insensitive. The excess volumes calculated from this equation should not be given too much significance since the Redlich–Kister relationship has no physical basis, particularly with respect to the complex Mg–Sb system.

Only very limited data for these alloys have been published. Greenaway (*3*) presented data for liquid Pb–Sb alloys that were obtained using a maximum bubble pressure technique, which works quite well for surface tension determinations but can be highly inaccurate for density measurements. His results show both very large positive and very large negative excess vol-

* Author to whom correspondence should be sent.

0021-9568/90/1735-0153$02.50/0

Table I. Experimental Data with Compositions Presented in Atom Fractions

metal or alloy	T, °C	ρ, g/cm^3	v, cm^3/mol	metal or alloy	T, °C	ρ, g/cm^3	v, cm^3/mol
pure In	826	6.538	17.561	0.90 In–0.10 Sb	473	6.716	17.200
	760	6.583	17.441		391	6.778	17.042
	690	6.630	17.318	0.10 Mg–0.90 Sb	957	5.915	18.935
	620	6.677	17.197		905	5.943	18.848
	560	6.719	17.089		849	5.970	18.762
	473	6.785	16.924		803	5.991	18.697
	395	6.844	16.778		752	6.015	18.622
	298	6.917	16.599		707	6.039	18.546
	193	6.999	16.405	0.20 Mg–0.80 Sb	953	5.512	18.552
pure Mg	906	1.500	16.209		903	5.528	18.499
	877	1.505	16.153		855	5.548	18.432
	825	1.517	16.030		800	5.575	18.343
	806	1.520	15.999		753	5.599	18.263
	752	1.532	15.867		705	5.622	18.191
	704	1.542	15.771	0.30 Mg–0.70 Sb	958	5.219	17.727
	670	1.550	15.683		908	5.242	17.649
pure Pb	1016	9.866	21.001		853	5.269	17.561
	950	9.923	20.880		803	5.287	17.501
	902	9.974	20.773	0.40 Mg–0.60 Sb	954	4.822	17.168
	855	10.024	20.670		904	4.846	17.081
	797	10.090	20.535		852	4.878	16.967
	652	10.259	20.197		807	4.916	16.837
	595	10.323	20.070	0.80 Mg–0.20 Sb	995	2.695	16.250
	546	10.381	19.958		963	2.712	16.152
	501	10.437	19.852		913	2.731	16.039
	498	10.441	19.843		881	2.742	15.971
	449	10.500	19.732	0.90 Mg–0.10 Sb	952	2.124	16.031
	394	10.573	19.597		896	2.143	15.895
	343	10.635	19.481		852	2.156	15.795
pure Sb	898	6.353	19.163		805	2.171	15.684
	852	6.380	19.082	0.10 Pb–0.90 Sb	867	6.739	19.335
	800	6.408	19.001		802	6.783	19.209
	751	6.433	18.927		746	6.823	19.097
	694	6.465	18.832		693	6.856	19.006
	645	6.493	18.751		648	6.887	18.919
0.10 In–0.90 Sb	852	6.362	19.028	0.20 Pb–0.80 Sb	853	7.128	19.477
	802	6.393	18.937		797	7.167	19.372
	751	6.426	18.840		741	7.206	19.268
	705	6.453	18.761		692	7.245	19.165
	646	6.489	18.657		642	7.283	19.063
0.20 In–0.80 Sb	840	6.367	18.905	0.30 Pb–0.70 Sb	864	7.500	19.650
	802	6.389	18.839		787	7.554	19.510
	747	6.420	18.749		626	7.680	19.191
	703	6.448	18.667		521	7.761	18.990
	642	6.487	18.552	0.40 Pb–0.60 Sb	851	7.880	19.787
0.50 In–0.50 Sb	827	6.370	18.570		770	7.944	19.627
	764	6.414	18.446		709	7.988	19.519
	710	6.446	18.349		608	8.071	19.319
	649	6.482	18.248		513	8.153	19.126
	601	6.509	18.173	0.50 Pb–0.50 Sb	855	8.229	19.987
	540	6.546	18.070		785	8.290	19.840
0.60 In–0.40 Sb	701	6.468	18.180		687	8.376	19.637
	647	6.500	18.092		603	8.450	19.463
	616	6.519	18.039		523	8.525	19.292
	572	6.548	17.958		466	8.575	19.181
	534	6.574	17.889	0.70 Pb–0.30 Sb	845	8.965	20.253
0.70 In–0.30 Sb	699	6.492	18.007		772	9.040	20.084
	646	6.523	17.922		684	9.130	19.886
	604	6.553	17.838		582	9.241	19.648
	548	6.589	17.741	0.80 Pb–0.20 Sb	858	9.316	20.406
	508	6.615	17.672		779	9.397	20.230
0.80 In–0.20 Sb	821	6.427	18.081		701	9.477	20.059
	735	6.486	17.917		591	9.596	19.810
	646	6.545	17.755		500	9.703	19.592
	566	6.601	17.605	0.90 Pb–0.10 Sb	805	9.726	20.425
	488	6.655	17.462		727	9.808	20.254
	427	6.696	17.354		645	9.893	20.080
0.90 In–0.10 Sb	820	6.483	17.819		552	9.993	19.880
	723	6.546	17.648		410	10.196	19.484
	640	6.599	17.504		339	10.291	19.304
	551	6.662	17.340				

umes; it is unlikely that these are correct. Crawley (*4*) also published data for the Pb–Sb system but only in the region of dilute Sb. The authors are aware of no other volumetric information for the In–Sb and Mg–Sb alloys.

Due to the high temperatures and materials problems for these measurements, experimental errors are relatively large as compared to those for organic systems. Uncertainties arose mainly from the balance readings and bob calibrations that

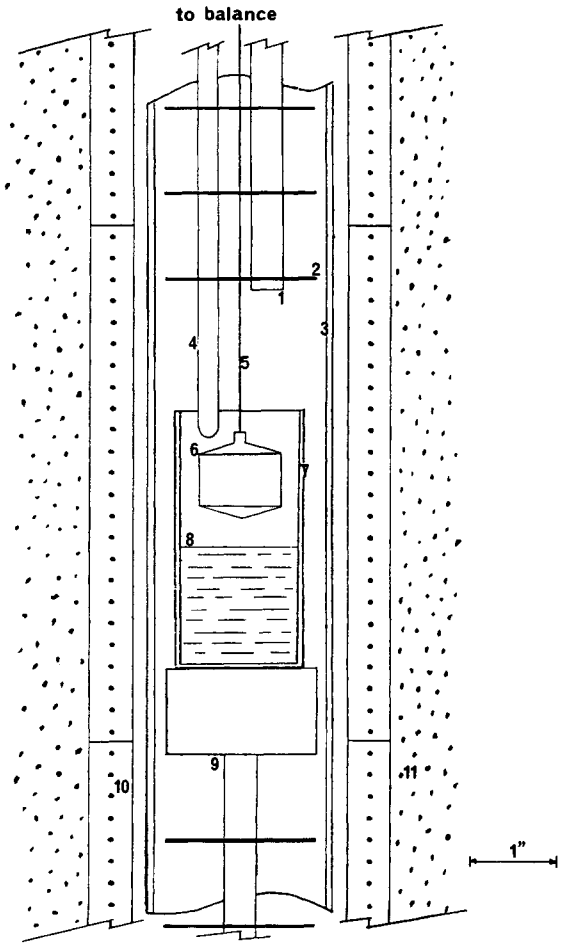

Figure 1. Experimental chamber: (1) metal addition tube; (2) heat shields; (3) quartz furnace tube; (4) thermocouple and protective sleeve; (5) suspension wire; (6) bob; (7) alumina crucible; (8) melt; (9) movable crucible support (in lower position); (10) semicylindrical heating elements; (11) insulation.

Table II. Linear Least-Squares Fits of Experimental Molar Volume Data with Compositions Presented in Atom Fractions: v (cm³/mol) ±0.1% = aT (°C) + b

metal or alloy	a, 10^{-3} cm³/(mol °C)	b, cm³/mol
pure In	1.828	16.057
pure Mg	2.226	14.197
pure Pb	2.290	18.703
pure Sb	1.613	17.712
0.10 In–0.90 Sb	1.803	17.490
0.20 In–0.80 Sb	1.776	17.416
0.50 In–0.50 Sb	1.724	17.134
0.60 In–0.40 Sb	1.748	16.958
0.70 In–0.30 Sb	1.772	16.771
0.80 In–0.20 Sb	1.846	16.563
0.90 In–0.10 Sb	1.807	16.342
0.10 Mg–0.90 Sb	1.532	17.465
0.20 Mg–0.80 Sb	1.491	17.145
0.60 Mg–0.70 Sb	1.474	16.312
0.40 Mg–0.60 Sb	2.240	15.044
0.80 Mg–0.20 Sb	2.427	13.826
0.90 Mg–0.10 Sb	2.354	13.789
0.10 Pb–0.90 Sb	1.894	17.691
0.20 Pb–0.80 Sb	1.962	17.807
0.30 Pb–0.70 Sb	1.935	17.982
0.40 Pb–0.60 Sb	1.948	18.131
0.50 Pb–0.50 Sb	2.078	18.209
0.70 Pb–0.30 Sb	2.296	18.313
0.80 Pb–0.20 Sb	2.267	18.465
0.90 Pb–0.10 Sb	2.416	18.504

resulted in errors of approximately ±0.1% in the densities and molar volumes. This corresponds to errors of nearly ±0.02 cm³/mol in the excess volumes. For the Mg–Sb alloys, however, uncertainties may be as large as ±0.05 cm³/mol. The compositions presented in Table I are considered to be accurate to a mole fraction of ±0.0005.

The large, negative excess volumes for the Mg–Sb system are common to intermetallic compound-forming systems and

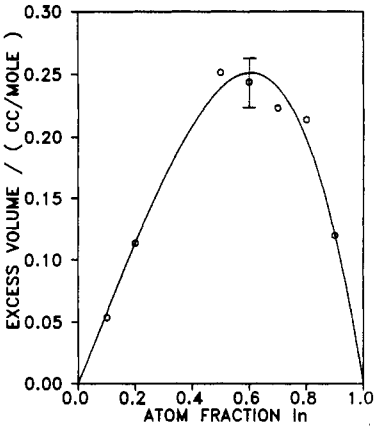

Figure 2. Excess volumes of liquid indium–antimony alloys at 650 °C: (O) experimental data; (—) empirical fit.

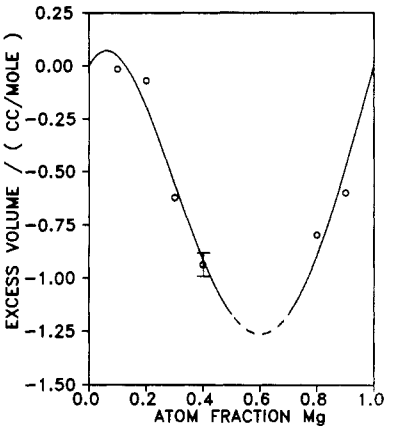

Figure 3. Excess volumes of liquid magnesium–antimony alloys at 850 °C: (O) experimental data; (—) empirical fit; (- -) inaccessible region.

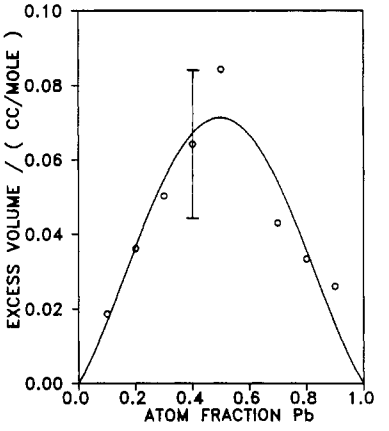

Figure 4. Excess volumes of liquid lead–antimony alloys at 650 °C: (O) experimental data; (—) empirical fit.

Table III. Empirical Fits of Excess Volume Data: v^{EX} ±0.02 (cm³/mol) = $x_A x_B(A + B(x_A - x_B) + C(x_A - x_B)^2)$

alloy, A–B	T, °C	A, cm³/mol	B, cm³/mol	C, cm³/mol
In–Sb	650	0.956	0.441	0.051
	750	0.961	0.381	0.190
Mb–Sb	850	−4.676	−3.652	3.528
	900	−4.599	−3.494	3.357
Pb–Sb	650	0.285	−0.005	−0.164
	750	0.318	−0.009	0.085

are consistent with the excess volumes obtained for Mg-Bi, Mg-Pb, and Mg-Sn alloys (5-7). Notice also that the minimum in the excess volume curve corresponds rather well with the stoichiometry of the Mg_3Sb_2 compound.

Though the In-Sb system also shows evidence of the formation of a weak 1:1 compound in the liquid phase (8), our excess volumes are positive. This could have two explanations: either the physical interactions are more important than the chemical interactions or the volume of the compound is larger than the sum of the volumes of its components. The former explanation seems to be more likely for this system since the maximum in the curve occurs far from the equimolar concentration. Also, our excess volume model (1) predicts an equimolar excess volume of about 0.22 cm^3/mol compared to the experimental result, 0.24 cm^3/mol. This model was developed for non-compound-forming alloys and seems to work reasonably well for systems that exhibit positive excess volumes.

The solid-liquid phase diagram for the Pb-Sb system is that of a simple eutectic (9). The physical interactions of these types of alloys generally lead to positive excess volumes as observed here. Our model (1) predicts an equimolar excess volume of 0.08 cm^3/mol, which agrees nearly exactly with experiment.

Literature Cited

(1) Hansen, A. R.; Kaminski, M. A.; Lira, C. T.; Eckert, C. A. *Ind. Eng. Chem. Res.* **1989**, *28*, 97.
(2) Bockris, J.; White, J.; Mackenzie, J. *Physicochemical Measurements at High Temperature*; Butterworths: London, 1959.
(3) Greenaway, H. T. *J. Inst. Metals* **1948**, *74*, 133.
(4) Crawley, A. I. *Trans. TMS-AIME* **1968**, *242*, 859.
(5) Gebhardt, E.; Becker, M.; Dorner, S. *Z. Metallkd.* **1955**, *46*, 669.
(6) Grant, R. The Liquid State Densities of Metals, Alloys and Intermetallic Compounds. Ph.D. Thesis, Syracuse University, 1968.
(7) Faxon, R. Density Studies of Liquid Metal Systems. Ph.D. Thesis, Syracuse University, 1966.
(8) Howell, W. J.; Lira, C. T.; Eckert, C. A. *AIChE J.* **1988**, *34*, 1477.
(9) Hultgren, R.; Desai, P. D.; Hawkin, D. T.; Greiser, M.; Kelley, K. K. *Selected Values of Thermodynamic Properties of Binary Alloys*; American Society for Metals: Metals Park, OH, 1973.

Received for review April 19, 1989. Accepted November 7, 1989. We are grateful for the financial support of the Standard Oil Co. (Indiana) and the Link Foundation.

Limiting Activity Coefficients from an Improved Differential Boiling Point Technique

D. Mark Trampe[†] and Charles A. Eckert[*,‡]

Department of Chemical Engineering, University of Illinois, Urbana, Illinois 61801

Infinite dilution activity coefficients were measured for 54 systems with an improved differential boiling point apparatus. Following the suggestions of Scott, a radical new boiler design is used that exhibits better temperature stability, allowing more precise and accurate data to be measured. The results are compared to available literature data. The temperature dependence of γ^∞ was also studied and found to be reasonable. Estimates of the partial molar excess enthalpy at infinite dilution are reported.

Introduction

The direct experimental determination of limiting activity coefficients was first proposed by Gatreaux and Coates (2). Through the years, advancements in boiler design and temperature measurement have increased the precision, accuracy, and range of applicability of the differential boiling point technique. The experimental apparatus first employed was that of the ebulliometer (3-5). The ebulliometers were of the Swietoslawski type, with use of the principle of the Cottrell pump. Recently, Scott (1) has introduced a radical change in the design of the apparatus, incorporating a round-bottom flask with high-speed stirring. These changes significantly reduced the temperature fluctuations. Also, with the use of a larger charge of solvent, composition errors are reduced and data can be obtained for systems of higher relative volatility. Further modifications to minimize leak problems and reduce maintenance have since been made and will be presented here. Data from use of the original Scott design as well as the modified apparatus will be presented and discussed.

To determine γ^∞ from dilute T-x data, the following expression is used:

$$\gamma_1^\infty = \{\phi_1^{(P_2^s)}[P_2^s - (1 - P_2^s v_2/RT + (P_2^s/\phi_2^s)(\partial\phi_2/\partial P)_T) \times (dP_2^s/dT)(\partial T/dx_1)_p^\infty]\}/\{P_1^s\phi_1^s \exp(v_1(P_2^s - P_1^s)/RT)\} \quad (1)$$

The rigorous derivation is given by Newman (6). Fugacity coefficients were determined from the volume explicit virial equation truncated after the second term. The second virial coefficients are obtained from experimental measurement (7) or estimated by the method of Hayden and O'Connell (8). Saturation pressures and liquid molar volumes are calculated from standard correlations as outlined by Trampe (9). The quantity that is determined experimentally is $(\partial T/\partial x_1)_p^\infty$, the limiting slope of the isobaric T-x data.

Apparatus

The boiler design initially used was that of Scott (1) as shown in Figure 1. The boilers are 500-mL round-bottom flasks fitted with high-speed stirrers driven with Bodine 1800 rpm synchronous motors. A quartz thermometer probe (Hewlett-Packard, Model 2804A) is immersed in mineral oil in the thermowell attached to the top of the flask. The thermowell is completely vacuum-jacketed and silvered to reduce heat losses and is connected to a reflux condenser containing ethylene glycol at -20 °C. Condensate is returned to the boiling flask with a capillary tube. Heat is supplied to the boiling flask with a Glas-Col heating mantle. This design was found to give much improved temperature stability over the previous ebulliometer apparatus. Depending on experimental conditions, the temperature stability approached the precision of the quartz thermometer, 0.0001 °C. However, leak problems often occurred with the high-speed stirrers, and under heavy use, maintenance of the stirrer become troublesome. To rectify these problems, the Scott apparatus was modified by incorporating magnetic

* Author to whom correspondence should be addressed.
† Present address: Union Carbide Corp. Bound Brook, NJ 08805.
‡ Present address: School of Chemical Engineering, Georgia Institute of Technology, Atlanta, GA 30332-0100.

0021-9568/90/1735-0156$02.50/0